



## Adsorption of Aqueous Glyphosate N-Phosphonomethylglycine by Manganese Oxides/Mesoporous Silica SBA-15 Composite at High Salinity Condition

HAO CUI, QIN LI, YAN QIAN, QIU ZHANG and JIANPING ZHAI\*

State Key Laboratory of Pollution Control and Resource Reuse and School of the Environment, Nanjing University, Nanjing 210093, P.R. China

\*Corresponding author: Tel/Fax: +86 25 83592903; E-mail: jpzhai@nju.edu.cn

(Received: 18 June 2011;

Accepted: 17 January 2012)

AJC-10973

Glyphosate N-phosphonomethylglycine (PMG) is the broad-spectrum herbicide used commonly around the world and the main feature of its production wastewater is high salinity. In this paper, the glyphosate removal by manganese-oxides-coated mesoporous silica SBA-15 ( $\text{MnO}_2/\text{SBA-15}$ ) under high background salinity conditions was examined. A chemical precipitation method was employed for  $\text{MnO}_2$  coating on an ordered mesoporous silica SBA-15 template to obtain a significantly enlarged BET surface area of the adsorbent, which was  $963 \text{ m}^2/\text{g}$ . The maximum glyphosate uptake capacity for  $\text{MnO}_2/\text{SBA-15}$  was found to be about  $300 \text{ mg/g}$ . The Langmuir equilibrium model was found to be suitable for describing the adsorption. Kinetic study showed that the adsorption fitted a pseudo-second-order kinetic model. The effects of different parameters such as pH and coexisted ions were also studied. The results also indicate the potential of adsorbents prepared by coating manganese oxides on porous materials *via* chemical precipitation in removing glyphosate from high-salinity wastewater.

**Key Words:** Manganese oxides,  $\text{MnO}_2/\text{SBA-15}$ , Glyphosate N-phosphonomethylglycine, High salinity, Adsorption.

### INTRODUCTION

Glyphosate N-phosphonomethylglycine (PMG) is a highly effective broad-spectrum, post-emergence and non-selective herbicide that is widely used in agriculture worldwide<sup>1,2</sup>. Many manufactures and reports claim that the use of glyphosate N-phosphonomethylglycine is safe for the environment<sup>3</sup>, but recent studies have showed that PMG may alter several vital biochemical processes in plants and microorganisms<sup>4,5</sup>, increase the mobility and bioavailability of some soil metal and correspondingly increase its environmental risk<sup>6</sup>. The United States Environmental Protection Agency (USEPA) has set maximum contaminant level (MCL) of  $700 \mu\text{g/L}$  for drinking water.

Glyphosate N-phosphonomethylglycine production industries generate large quantities of high salinity wastewater. Various treatment processes have been investigated to reduce glyphosate concentrations in water and to minimize the potential health risks, including electrooxidation<sup>7</sup>, biotreatment<sup>8,9</sup>, electric field-assisted biosorption<sup>10</sup>, nanofiltration<sup>11</sup> and photodegradation<sup>12</sup>. Among the problems encountered in the use of these techniques are high investment and operation cost. Adsorption is an ideal and appropriate technique because of its simplicity and cost effectiveness. PMG has three groups (amino, carboxylate and phosphonate) that enabled it to coordinate strongly to mineral surfaces<sup>13-15</sup>. It is commonly

believed that the formation of surface complexes through the phosphonate group is predominant, while the amine and carboxylate groups remain relatively free from complexation<sup>16,17</sup>. Adsorption of PMG on natural materials such as goethite<sup>16,18,19</sup>, manganite<sup>20,21</sup> and aluminum hydroxides<sup>22</sup> has been reported. However, high salt content in wastewater is known to significantly reduce the treatment efficiency of these natural adsorbents. Several materials have been synthesized and investigated for their glyphosate adsorption capacity such as MgAl-layered double hydroxides<sup>23</sup> and  $\text{Ni}_2\text{Al}_2\text{O}_3$  layered double hydroxide<sup>24</sup>, with adsorption capacity around 30 and  $200 \text{ mg/g}$ , respectively. However, there is still scope for improving the sorption capacity and simplifying the adsorbent preparation.

Many low cost porous materials, such as activated carbon, amorphous silica and some clay minerals, would be used as the template to enlarge the surface area of the adsorbent. These low cost porous materials, however, have both microporous and mesoporous structure, which would disturb the investigation of the adsorption of glyphosate by the adsorbent. Mesoporous material contains pores with diameters between 2 and 50 nm, which allows a smooth diffusion of molecules in the pores<sup>25</sup>. Shin *et al.*<sup>26</sup> have found that, compared with activated alumina, Al-impregnated mesoporous materials show fast adsorption kinetics as well as high adsorption capacities. It

was also reported that, the pores SBA-15 can be adjusted from 2-10 nm in a narrow diameter distribution region simply by changing the experimental conditions<sup>27</sup>. Therefore mesoporous silica SBA-15 was chosen as the template in order to clearly investigate the alterations after coating of MnO<sub>2</sub> into the channels and the adsorption performance of PMG on ordered mesoporous materials.

This study, therefore, synthesized a novel MnO<sub>2</sub>/SBA-15 composite adsorbent for effective PMG removal from waters with greatly enhanced surface area achieved by a chemical precipitation process of MnO<sub>2</sub> on an ordered SBA-15 template. The adsorption of PMG by the MnO<sub>2</sub>/SBA-15 composite from aqueous solutions was investigated as a function of the contact time, initial PMG concentration, ionic strength, pH value and coexisted anions of the aqueous solution.

## EXPERIMENTAL

Surfactant pluronic P123, *i.e.*, triblock poly(ethylene oxide)-poly(propylene oxide)-poly(ethylene oxide) (PEO<sub>20</sub>PPO<sub>70</sub>PEO<sub>20</sub>), was employed as the structure-directing agent for SBA-15 and tetraethoxysilane TEOS; (CH<sub>3</sub>-CH<sub>2</sub>O)<sub>4</sub>Si. have been employed as silica precursors. PMG from Fluka was used in adsorption experiments. All reagents were of analytical grade purchased from Aldrich.

**Sample preparation:** Preparation of SBA-15 was performed at State Key Laboratory of Pollution Control and Resources Reuse, Nanjing University, using the method reported by Kim *et al.*<sup>28</sup>.

The manganese dioxide coated mesoporous silica SBA-15 (MnO<sub>2</sub>/SBA-15) was prepared by a chemical precipitation process. 5 g SBA-15 was immersed in 50 mL of MnCl<sub>2</sub> solution at various concentrations and the pH was adjusted to 3.3. The suspension was vigorously stirred at room temperature with no pH control. Meanwhile 1.7 g of KMnO<sub>4</sub> was added to the suspension, immediately making the solution dark brown, which indicated the formation and precipitation of MnO<sub>2</sub>:



Finally, the suspension was filtered, washed with high-pure water and dried at 105 °C for 4 h.

The MnO<sub>2</sub>/SBA-15 composite was characterized by transmission electron microscopy (TEM) to evaluate the alterations of the surface and channels, whereas the surface area was calculated using the Brunauer-Emmett-Teller method.

**Batch adsorption experiments:** Batch adsorption experiments were conducted to examine the effects of adsorbent dose, contact time, initial PMG concentration, ionic strength, solution pH, as well as coexisted anions on adsorption performance. Single runs were carried out by stirring 200 mg of MnO<sub>2</sub>/SBA-15 composite in 25 mL of aqueous PMG solutions at 150 rpm and 25 °C. A preliminary kinetic test revealed that adsorption equilibrium of PMG on MnO<sub>2</sub>/SBA-15 composite was completely achieved within 24 h under the experimental conditions. Therefore, an equilibrium time of 24 h was adopted for all the adsorption tests. Mixtures were filtered with a syringe filter of 0.22 μm and the final solutions were collected. The PMG concentrations in both the initial and final solutions were evaluated UV-VIS spectroscopy and the absorbance was measured

around 243 nm<sup>23</sup>. The typical experimental error was kept lower than 5 % for all the experimental results.

## RESULTS AND DISCUSSION

**Optimization and surface characterization:** Coating MnO<sub>2</sub> on SBA-15 could not only increase the amount of active sites but also affect the micro-porous structure of SBA-15, which play an important role in the sorption process. Thus it is necessary to determine the optimal amount of MnO<sub>2</sub> that coated onto the SBA-15. The modified samples obtained at various concentrations (0.2, 0.3, 0.4, 0.6 mol/L) of MnCl<sub>2</sub> solution were investigated in batch adsorption experiment.

As shown in Fig. 1, the adsorption capacity of the MnO<sub>2</sub>/SBA-15 composite increases with the increase of the quantity of the MnO<sub>2</sub> coated on SBA-15 from 0.2-0.4M MnCl<sub>2</sub> and decreased with the increase of the quantity of the MnO<sub>2</sub> coated on SBA-15 from 0.4-0.6M MnCl<sub>2</sub>. The adsorption capacities of the coated SBA-15 obtained with a 0.4M MnCl<sub>2</sub> solution are higher than those achieved with other coated SBA-15 and at least ten times greater than those of uncoated SBA-15. Therefore, this MnO<sub>2</sub>/SBA-15 composite specimen was chosen as the sample in the following characterization and batch adsorption experiment. The amount of manganese on the surface of the MnO<sub>2</sub>/SBA-15 composite, measured through acid digestion analysis was approximately 62.4 mg Mn/g MnO<sub>2</sub>/SBA-15 composite.

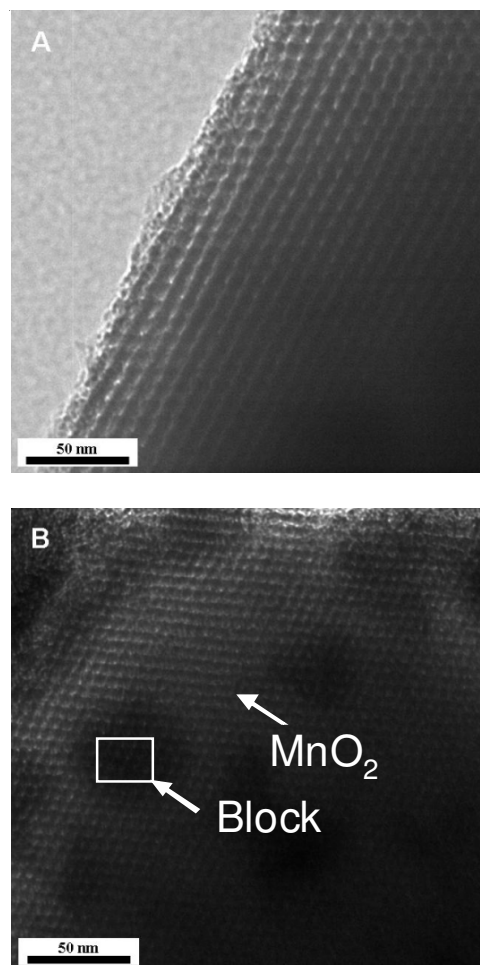


Fig. 1. TEM images of (A) uncoated SBA-15;(B) MnO<sub>2</sub>/SBA-15 composite

Microstructure of SBA-15 and MnO<sub>2</sub>/SBA-15 were investigated by TEM technique (Fig. 2A-B). TEM images evidenced that the well-ordered hexagonal structure of SBA-15 is maintained during the incorporation of MnO<sub>2</sub> chains into the channels. The black dots marked by the arrows were the MnO<sub>2</sub> forming within the channels of SBA-15 and the dark areas marked by the rectangle were the channels blocked by MnO<sub>2</sub>. The BET surface areas were 1012 and 963 m<sup>2</sup>/g for SBA-15 and MnO<sub>2</sub>/SBA-15, respectively, indicating the heap of MnO<sub>2</sub> within some channels.

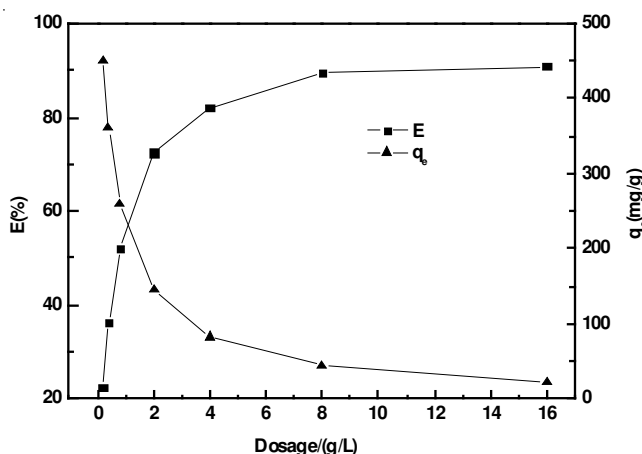


Fig. 2. Adsorption of PMG on MnO<sub>2</sub>/SBA-15 composite as a function of adsorbent dosage. PMG initial concentration = 400 mg/L; ionic strength = 1M NaCl; T = 298 K; pH = 4.0

**Amount of adsorbent:** Fig. 3 shows the effect of adsorbent dose on the removal of PMG at pH 4 and initial PMG concentration of 400 mg/L for 24 h. At 0.2 g/L of the adsorbent dose, 14.7 % of PMG was removed and gradually increases up to 84.1 % at 8 g/L of adsorbent and then continued to increase at lower speeds from 84.1-86.2 % at 16 g/L of adsorbent. Therefore, 8 g/L MnO<sub>2</sub>/SBA-15 is used in the following tests as the optimum adsorbent amount. The increase of the sorbent dosage leads to the decrease in  $q_e$  as there are too many adsorbent for the limited amount of PMG. And the PMG removal percentage increases with the dosage until equilibrium<sup>29</sup>. The saturation adsorbent capacity is fixed.

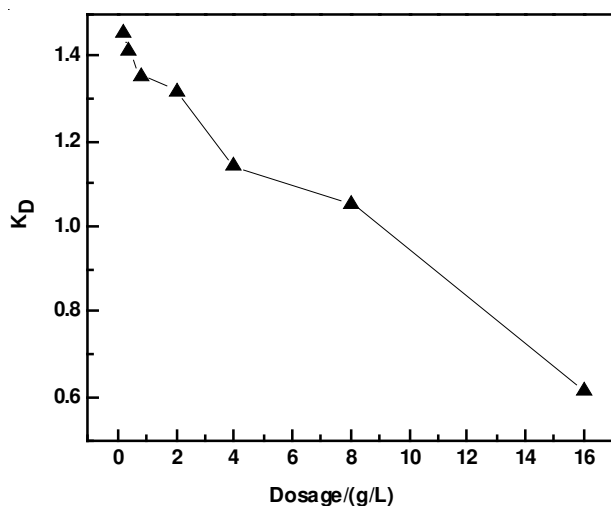


Fig. 3. Plot of  $K_D$  value as a function of adsorbent dosage

A distribution coefficient  $K_D$ , which reflects the binding ability between the adsorbent surface and PMG, was showed in Fig. 4.  $K_D$  is dependent on pH of the solution and type of surface of the adsorbent<sup>30</sup>. The distribution coefficient values of PMG adsorbed on MnO<sub>2</sub>/SBA-15 composite was computed using the following equation<sup>31</sup>:

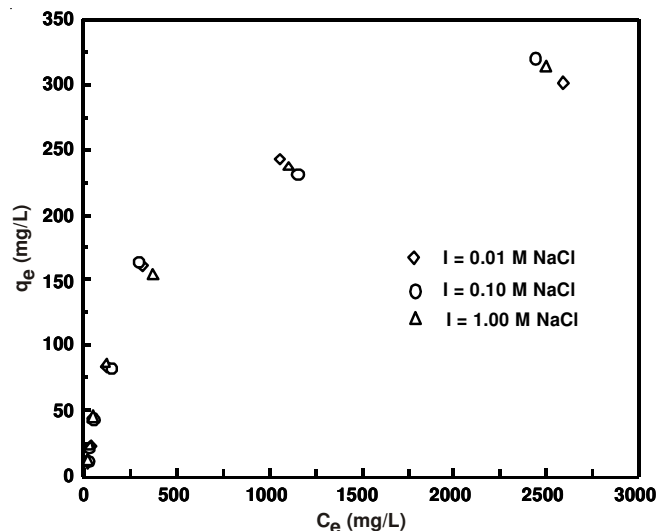


Fig. 4. Sorption isotherms of PMG by MnO<sub>2</sub>/SBA-15 composite at three levels of ionic strength (0.01, 0.10 and 1.00 M NaCl), pH = 4.0, adsorbent dosage = 8 g/L, PMG initial concentration at 100, 200, 400, 800, 1600, 3000, 5000 mg/L

$$K_D = \frac{C_s}{C_w} (\text{m}^3/\text{kg}) \quad (1)$$

where  $C_s$  is the concentration of PMG on the solid particles (mg/kg) and  $C_w$  is the equilibrium concentration in water solution (mg/m<sup>3</sup>). If the surface of the adsorbent is homogeneous, the  $K_D$  values would not change with the adsorbent dosage<sup>31</sup>. As illustrated in Fig. 4, the  $K_D$  value decreased with an increase in adsorbent dose. It implies that the surface of the MnO<sub>2</sub>/SBA-15 composite is heterogeneous.

**Sorption isotherms and influence of ionic strength:** Generally, for conventional adsorbents such as activated-carbon, glyphosate adsorbs very strongly in distilled water but has a much lower capacity in high salinity water. Fig. 5 shows the adsorption isotherms of PMG onto MnO<sub>2</sub>/SBA-15 composite covering a wide range of ionic strengths (0.01, 0.10 and 1.00 M) and PMG concentrations. As illustrated in Fig. 5, the maximum uptake capacities for PMG at 0.01, 0.10 and 1.00 M ionic strengths are about 298, 312 and 285 mg/g, respectively. The adsorption of PMG occurs over a wide range of ionic strength and the maximum adsorption took place at 1 M. Also, adsorption was always higher at any ionic strength for MnO<sub>2</sub>/SBA-15 when compared to plain SBA-15. This will have an implication in the treatment of PMG production wastewater where the ionic strength is around 1 M. In depth studies have been done to establish the mechanism of adsorption of PMG onto coated SBA-15 which is discussed in the following sections.

Both the Langmuir eqn. 2 and the Freundlich equations eqn. 3 were used to describe the adsorption isotherms.

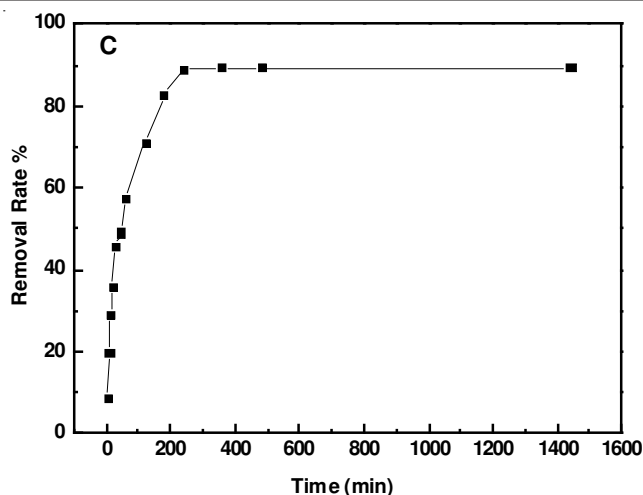


Fig. 5. Dynamics for PMG removal by MnO<sub>2</sub>/SBA-15 composite. PMG initial concentration = 400 mg/L; ionic strength = 1M NaCl; adsorbent dosage = 8 g/L; T = 298 K; pH = 4.0

$$\text{Langmuir: } Q_e = \frac{K_L Q_m C_e}{1 + K_L C_e} \quad (2)$$

$$\text{Freundlich: } Q_e = K_F C_e^{\frac{1}{n}} \quad (3)$$

where  $C_e$  (mg/L) is the equilibrium concentration of PMG,  $q_e$  (mg/g) the amount adsorbed under equilibrium,  $q_m$  (mg/g) the theoretical maximum adsorption capacity of the adsorbent for PMG,  $K_L$  (L/mg) a Langmuir binding constant related to the energy of adsorption,  $K_F$  and  $n$  the Freundlich empirical constants.

Table-1 shows the Langmuir and Freundlich isotherm constants. It can be seen that the Langmuir shows significantly higher correlations ( $R^2 \geq 0.99$ ) than the Freundlich model. Because the Langmuir model is based on the physical hypothesis that the maximum adsorption capacity consists of a monolayer adsorption, it is evident that the adsorption of PMG by MnO<sub>2</sub>/SBA-15 composite is a monolayer adsorption. The theoretical maximum adsorption capacities ( $q_m$ ) at the three ionic strengths (0.01, 0.10 and 1.00 M) are about 297.6, 299.6 and 307.4 mg/g, respectively, which are in good accordance with experimental data.

I (mol/L)	Langmuir model			Freundlich model		
	$Q_m$ (mg/g)	$K_L$ (L/g)	$R^2$	$K_F$	$n$	$R^2$
0.01	297.6	0.0036	0.9997	3.60	1.66	0.9637
0.10	299.6	0.0035	0.999	3.45	1.63	0.9596
1.00	307.4	0.0032	0.9993	3.34	1.62	0.9543

**Kinetic studies:** Influence of contact times up on the adsorption of PMG were recorded at adsorbate concentration of 400 mg/L as shown in Fig. 6. Adsorption of PMG increased fast in the first 3 h and then decreased and attained equilibrium at 4 h, indicating that the adsorption sites in the pores of the SBA-15 are not well exposed. Kinetic data of PMG sorption onto MnO<sub>2</sub>/SBA-15 were studied with pseudo-first and

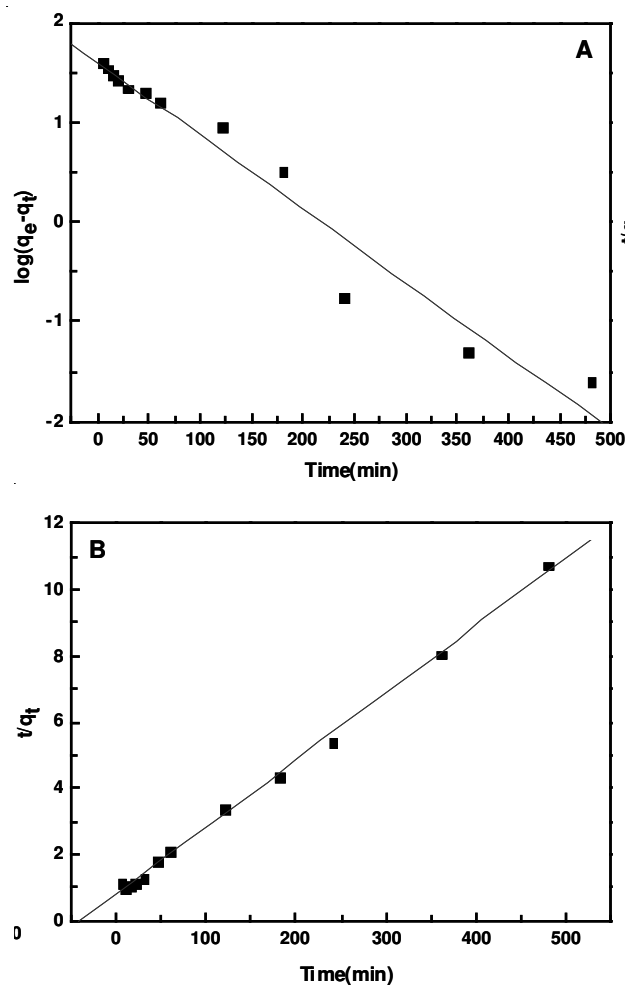


Fig. 6. (A) Pseudo-first-order kinetics of PMG sorption by MnO<sub>2</sub>/SBA-15 composite. B: pseudo-second-order kinetics of PMG sorption by MnO<sub>2</sub>/SBA-15 composite

pseudo-second order kinetic models. The mathematical representations of models are given in eqns. 4 and 5, respectively.

$$\lg (q_e - q) = \lg q_e - K_1 t \quad (4)$$

$$\frac{t}{q} = \left( \frac{1}{K_2 q_e^2} \right) + \left( \frac{t}{q_e} \right) \quad (5)$$

where  $K_1$  (min<sup>-1</sup>) represents the rate constant,  $q_e$  (mg/g) the amount of PMG adsorbed on the adsorbent surface at equilibrium,  $K_2$  the pseudo-second-order rate constant (g mg<sup>-1</sup> min<sup>-1</sup>) and  $q$  (mg/g) the amount of PMG adsorbed at any time  $t$  (min).

The adsorption rate constant ( $K_1$ ) in 480 min for PMG adsorption was calculated from the slope of the linear plot of  $\lg (q_e - q_t)$  versus time (Fig. 7A).  $K_2$  could be determined from the slope and interception by plotting  $t/q$  versus  $t$  (Fig. 7B). The rate constants obtained from first- and second-order pseudo-kinetic models are given in Table-2. The entire kinetic data fitted well with pseudo-second-order reaction rate model, which is evident from the higher correlation coefficient values. Also, the adsorption capacities calculated by the model are close to those results obtained from experiments. These results suggest that chemical adsorption involving valency forces may limit the PMG adsorption process.



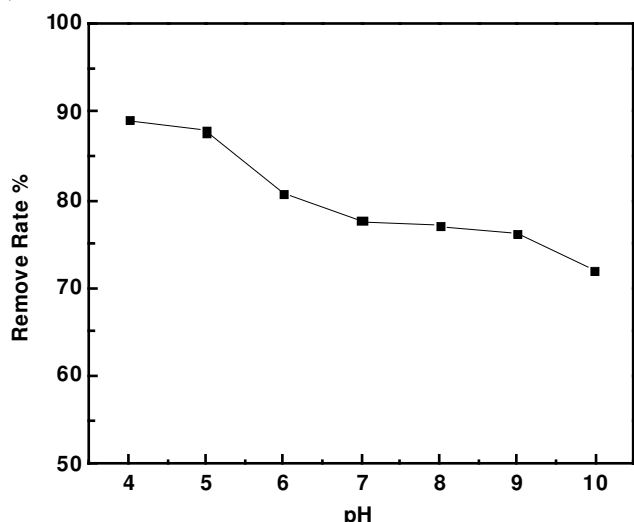


Fig. 7. Effect of solution pH on PMG removal by MnO<sub>2</sub>/SBA-15 composite. PMG initial concentration = 400 mg/L; ionic strength = 1M NaCl; adsorbent dosage = 8 g/L; pH adjusted by HCl and NaOH solutions; the pH value is the pH of the solution at equilibrium

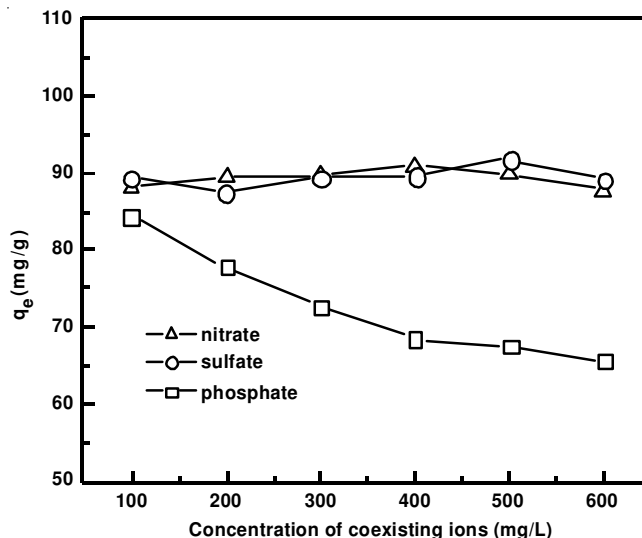
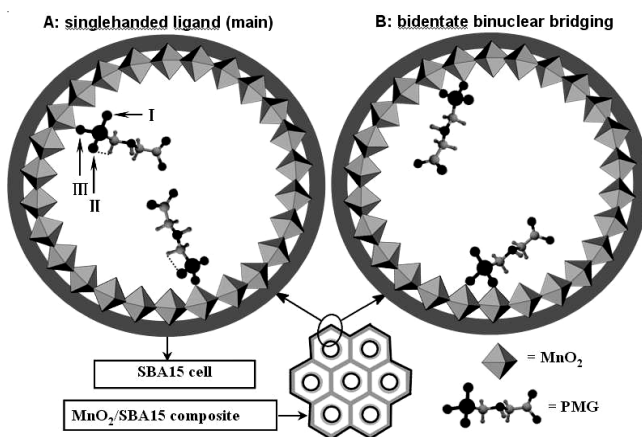


Fig. 8. Effect of coexisting anions (nitrate, sulfate and phosphate at the concentrations of 100, 200, 300, 400, 500 and 600 mg/L) on PMG removal by MnO<sub>2</sub>/SBA-15 composite. PMG initial concentration = 500 mg/L; ionic strength = 1M NaCl; pH = 4.0; adsorbent dosage = 8 g/L

TABLE-2 PARAMETERS OF KINETIC MODELS OF PMG ADSORPTION ONTO MnO <sub>2</sub> /SBA-15			
Pseudo-first-order model in 480 min			
q <sub>e</sub> exp (mg/g)	K <sub>1</sub> (min <sup>-1</sup> )	q <sub>e</sub> calcd. (mg/g)	R <sup>2</sup>
44.7	7.4 × 10 <sup>-3</sup>	38.34	0.9572
Pseudo-second-order model in 480 min			
q <sub>e</sub> exp (mg/g)	K <sub>2</sub> (g mg <sup>-1</sup> min <sup>-1</sup> )	q <sub>e</sub> calcd. (mg/g)	R <sup>2</sup>
44.7	5.07 × 10 <sup>-4</sup>	46.26	0.9977

**Influence of pH:** Generally, pH is an important factor affecting the adsorption process. Fig. 8 presents the PMG removal after adsorption at different initial pH values, ranging from 4-10. PMG adsorption was found to decrease with increasing pH values. When PMG get into the channels of MnO<sub>2</sub>/SBA-15 composite, there are essentially three types of phosphonate bonds responsible for the adsorption mechanisms, *i.e.*, uncomplexed P-O (I), intramolecularly hydrogen bonded P-O (II) and surface complexed P-O (III)<sup>16</sup>. Therefore, the proposed stoichiometries and structures of PMG-MnO<sub>2</sub> surface complexes could be described as **Scheme-I**, *i.e.*, single handed ligand between PMG and manganite (**Scheme-I-A**) and the bidentate binuclear bridging PMG-manganite complex (**Scheme-I-B**). The single handed ligand of PMG and manganite group would be easily affected by hydration while the bidentate binuclear bridging PMG-manganite group complex is independent of hydration process including pH conditions. Thus, the adsorption of PMG by MnO<sub>2</sub>/SBA-15 can be modeled as a chemical adsorption as single handed ligand between PMG and manganite.

**Effect of interfering anions:** Usually in wastewater many ions such as nitrate, sulfate and phosphate are present and these compete with PMG during adsorption. Fig. 9 shows the effect of these anions on the adsorption of PMG onto MnO<sub>2</sub>/SBA-15. The initial concentration of PMG was fixed (500 mg/L) whereas the concentration of sulfate, phosphate, chloride and nitrate was varied in the adsorption test. It can be seen that SO<sub>4</sub><sup>2-</sup> and NO<sub>3</sub><sup>-</sup> has not shown significant interference in PMG



**Scheme-I:** Proposed stoichiometries and structures of PMG-MnO<sub>2</sub> surface complexes

uptake. By contrast, the adsorption of PMG decreased with increase in phosphate concentration. This could be attributed to their competence with PMG for the active sites. This result is also evident for the assumption that PMG adsorption process was controlled by chemical process.

## Conclusion

In this study, manganese-oxide-coated mesoporous silica SBA-15 was prepared *via* chemical precipitation. The SBA-15 template supplied a large surface area of 963 m<sup>2</sup>/g for the coating of MnO<sub>2</sub>, which provided plentiful binding sites for PMG adsorption. The MnO<sub>2</sub>/SBA-15 composite is capable of maintaining a high PMG adsorption capacity under high salinity conditions (1M NaCl), with a maximum adsorption capacity of over 300 mg/g. The adsorption isotherms were well described by Langmuir model. It was found that the pseudo-second-order model better represented the sorption kinetics in the PMG adsorption, suggesting that the PMG adsorption process by MnO<sub>2</sub>/SBA-15 composite is controlled by chemical process. The adsorption of PMG by MnO<sub>2</sub>/SBA-

15 can be modeled as the formation of singlehanded ligand between PMG and manganite. The result indicates an important role of MnO<sub>2</sub>/SBA-15 composite as a potential adsorbent for removal of organophosphate and organophosphonate pollutants from high salinity wastewater.

### ACKNOWLEDGEMENTS

This work was supported by the Natural Science Foundation of China (Grants 51008154) and Resource Reuse of China and the Scientific Research Foundation of Graduate School of Nanjing University (Grants 2010CL07).

### REFERENCES

- J. Franz, M. Mao and J. Siroski, Glyphosate: A Unique Global Herbicide, ACS. Monograph, Vol. 189, (1997).
- A.T. Woodburn, *Pest Manage. Sci.*, **56**, 309 (2000).
- S.M. Carlisle and J.T. Trevors, *Water Air Soil Pollut.*, 39 (1988).
- C. Gasnier, C. Dumont, N. Benachour, E. Clair, M.-C. Chagnon and G.-E. S eralini, *Toxicology*, **262**, 184 (2009).
- L.G. Blackburn and C. Boutin, *Ecotoxicology*, **12**, 271 (2003).
- Y.-J. Wang, D.-M. Zhou, R.-J. Sun, L. Cang and X.-Z. Hao, *J. Hazard. Mater.*, **137**, 76 (2006).
- S.A. Neto and A.R. de Andrade, *Electrochim. Acta*, **54**, 2039 (2009).
- L.E. Hallas, W.J. Adams and M.A. Heitkamp, *Appl. Environ. Microbiol.*, **38**, 921 (1992).
- T.V. Shushkova, G.K. Vasilieva, I.T. Ermakova and A.A. Leontievsky, *Appl. Biochem. Microbiol.*, **45**, 599 (2009).
- N. Nomikou, P. Hughes and A.P. McHale, *J. Chem. Technol. Biotechnol.*, **81**, 1514 (2006).
- M. Xie, Z.Y. Liu and Y.H. Xu, *J. Hazard. Mater.*, **181**, 975 (2010).
- Y. Chen, F. Wu, Y. Lin, N. Deng, N. Bazhin and E. Glebov, *J. Hazard. Mater.*, **148**, 360 (2007).
- R.J. Hance, *J. Pestic. Sci.*, **7**, 363 (1976).
- S. Shoval and S. Yariv, *Clays Clay Miner.*, **27**, 19 (1979).
- R.L. Glass, *J. Agric. Food Chem.*, **35**, 497 (1987).
- J. Sheals, S. Sjöberg and P. Persson, *Environ. Sci. Technol.*, **36**, 3090 (2002).
- B.C. Barja and M.D. Afonso, *Environ. Sci. Technol.*, **39**, 585 (2005).
- G.M. Day, B.T. Hart, I.D. McKelvie and R. Beckett, *Environ. Technol.*, **18**, 781 (1997).
- J.S. McConnell and L.R. Hossner, *J. Agric. Food Chem.*, **33**, 1075 (1985).
- M. Ramstedt, C. Norgren, A. Shchukarev, S. Sjöberg and P. Persson, *J. Colloid. Interf. Sci.*, **285**, 493 (2005).
- C.M. Jonsson, P. Persson, S. Sjöberg and J.S. Loring, *Environ. Sci. Technol.*, **42**, 2464 (2008).
- W.E. Dubbin, G. Sposito and M. Zavarin, *Soil Sci.*, **165**, 699 (2000).
- F. Li, Y. Wang, Q. Yang, D.G. Evans, C. Forano and X. Duan, *J. Hazard. Mater.*, **125**, 89 (2005).
- A. Khenifi, Z. Derriche, C. Mousty, V. Pr evot and C. Forano, *Appl. Clay Sci.*, **47**, 362 (2010).
- Y. Yamada, O. Tanaike, T.T. Liang, H. Hatori, S. Shiraishi and A. Oya, *Electrochem. Solid-State Lett.*, **5**, 283A (2002).
- E.W. Shin, J.S. Han, M. Jang, S.H. Min, J.K. Park and R.M. Rowell, *Environ. Sci. Technol.*, **38**, 912 (2004).
- X. Feng, G. Yang, Y. Liu, W. Hou and J. Zhu, *J. Appl. Polym. Sci.*, **101**, 2088 (2006).
- J.M. Kim and G.D. Stucky, *Chem. Commun.*, 1159 (2000).
- A. Boualia, A. Mellah, T.T. Aissaoui, K. Menacer and A. Silem, *Appl. Clay Sci.*, **7**, 431 (1993).
- S.S. Tripathy, J.L. Bersillon and K. Gopal, *Sep. Purif. Technol.*, **50**, 310 (2006).
- L. Sigg, In ed.: S. Werner, Chemical Processes at the Particle Water-Interface, Aquatic Surface Chemistry, John Wiley & Sons, New York, p. 325 (1987).